Clays and Clay Minerals, Vol. 67, No. 5:410–418, 2019

THE EFFECTS OF OXYANION ADSORPTION ON REACTIVE OXYGEN SPECIES GENERATION BY TITANIUM DIOXIDE

Mary R. Arenberg and Yuji Arai*

[1]Department of Natural Resources and Environmental Sciences, University of Illinois at Urbana-Champaign, Urbana, IL 61801, USA

Abstract—The growing use of nano titanium dioxide (TiO_2) in consumer and agricultural products has accelerated its introduction into terrestrial environments, where its impact has not been documented extensively. TiO_2 toxicity arises primarily from its ability to photochemically generate reactive oxygen species (ROS), including hydrogen peroxide (H_2O_2). While common ligands in soil porewaters can either hinder or enhance the degradation of organic contaminants by TiO_2, their effects on ROS production by TiO_2 have not been understood clearly. The objective of this study was to assess the effect of phosphate (P) and nitrate on UV-irradiated anatase, nano-TiO_2. Accordingly, H_2O_2-generation kinetics experiments were conducted in UV-irradiated TiO_2 under environmentally relevant concentrations of the ligands (0, 50, 100, and 250 μM) and pH values (4.00 ± 0.02 and 8.00 ± 0.02) from 0–100 min. Under all conditions, H_2O_2 grew logarithmically and reached between 5.38 and 22.98 μM after 100 min. At pH 4.00 ± 0.02, H_2O_2 production was suppressed by P but not by nitrate. Conversely, at pH 8.00 ± 0.02, nitrate did not affect H_2O_2 concentration while P increased it. Non-specific, minimal adsorption of nitrate prevented interference with the photoreactivity of TiO_2. Due to the pH-dependent behavior of suspended TiO_2 and H_2O_2 degradation rates, specific adsorption of P on TiO_2 impeded its ability to produce H_2O_2 photochemically at pH 4.00 ± 0.02 but amplified it at pH 8.00 ± 0.02.

Keywords—Adsorption · Anatase · Nitrate · Phosphate · Photocatalysis · ROS · TiO_2

INTRODUCTION

Engineered nanomaterials (ENM) are utilized in various consumer products, including cosmetics, plastics, fuel additives, textiles, paints, coatings, dietary supplements, medical applications, etc. (Keller & Lazareva 2013; Manke et al. 2013; Sajid et al. 2015). During their production, use, and disposal each year, ~51,600 metric tons of ENMs are released into the soil globally (Keller & Lazareva 2013). Within terrestrial environments, ENMs have both beneficial and detrimental impacts (Gardea-Torresdey et al. 2014; Sajid et al. 2015). The positive effects of ENMs primarily involve increased yields of various crops and enhanced degradation of toxic chemicals (Ravichandran et al. 2010; Gardea-Torresdey et al. 2014). Conversely, the risks of ENMs include cyto- and genotoxicity to humans, animals, and plants as well as decreased crop biomass (Ghosh et al. 2010; Manke et al. 2013; Fu et al. 2014; Gardea-Torresdey et al. 2014; Sajid et al. 2015). These impacts vary widely depending on the type and concentration of the ENM and the type of organism exposed (Manke et al. 2013).

Titanium dioxide is one of the most common ENMs and is frequently released into the environment through cosmetic, agricultural, medicinal, and food-additive applications (Weir et al. 2012; Fu et al. 2014; Gondikas et al. 2014; Sajid et al. 2015). Unlike naturally occurring TiO_2 particles, TiO_2 environmental nanoparticles (ENPs) are manufactured to be homogeneous in size, shape, and structure. They also have smaller diameters and greater reactive surface area than natural TiO_2 (Bernhardt et al. 2010). The homogeneity, purity, and large reactive surface area make engineered TiO_2 NPs more reactive. Smaller particles become more photoreactive because of an increase in band-gap energies (Kavan et al. 1993). Their release into soil and water environments, in particular, is extensive because they are utilized in various agricultural applications, including soil remediation nano-technologies and nano-enabled pesticides, fertilizers, soil additives, and growth regulators (Gardea-Torresdey et al. 2014). Additionally, TiO_2 is added to the soil through the application of biosolids, which tend to have high concentrations of TiO_2 (10–70 mg kg^{-1}) (Keller & Lazareva 2013; Gardea-Torresdey et al. 2014). Consequently, soil TiO_2 concentrations can be significant. For instance, an exposure model predicted that nano-TiO_2 concentrations in Swiss soils fall between 0.4 and 4.8 μg kg^{-1}, depending on the extent of the emissions (Mueller et al. 2009). In the USA, soil nano-TiO_2 increases by 0.43–2.13 μg kg^{-1} y^{-1} across all soil types, and by 34.5–170 μg kg^{-1} y^{-1} in sludge-treated soils (Gottschalk et al. 2009).

Elevated TiO_2 concentrations in soils and porewater can lead to adverse effects. Past studies have reported that plant exposure to TiO_2 altered the chlorophyll content and antioxidative enzyme activities and led to Ti accumulation in fruit, roots, stems, and leaves (Servin et al. 2013; Gardea-Torresdey et al. 2014). Additionally, TiO_2 can negatively affect wheat growth and soil enzyme activity and lead to phytotoxicity and DNA fragmentation (Sajid et al. 2015).

Furthermore, TiO_2 toxicity may also detrimentally affect aquatic and terrestrial organisms, including arthropods, nematodes, and earthworms. The toxicity of anatase TiO_2 arises from its ability to generate reactive oxygen species when exposed to UV light (Ma et al. 2012). Reactive oxygen species cause oxidative stress to various soil organisms. While TiO_2 exposure can increase the feeding rates and catalase activities of the terrestrial arthropod *Porcellio scaber* (Drobne et al. 2009), it can also destabilize the cell membranes in these arthropods' isolated digestive glands (Valant et al. 2009). Moreover, the fertility and survival of nematode *Caenorhabditis elegans* was compromised by exposure to nano-TiO_2 (Wang et al. 2009). In fact, the degree of those effects were inversely correlated with the size of the TiO_2

* E-mail address of corresponding author: yarai@illinois.edu
DOI: 10.1007/s42860-019-00039-8

particle (Roh et al. 2010). Nano-TiO_2 with a diameter <30 nm can enter plant cell-wall pores and be taken up into the roots. In roots, TiO_2 can interrupt water flow and hydraulic potential. It can also be translocated from the roots into the leaves, where it influences pigments (i.e. chlorophyll, anthocyanin, and carotenoid) (Tan et al. 2018). Anatase TiO_2 accelerates the nitrogen metabolism of spinach by increasing the activities of nitrate reductase, glutamate dehydrogenase, glutamine synthase, and glutamic–pyruvic transaminase and by promoting the absorption of inorganic nitrogen and its subsequent conversion to organic forms (Yang et al. 2006). Finally, TiO_2 can bioaccumulate in earthworms and lead to oxidative stress, DNA and mitochondrial damage, and inhibition of cellulase (Hu et al. 2010).

Many of these risks arise because TiO_2 generates reactive oxygen species (ROS) under exposure to UV-light (Skocaj et al. 2011; Fu et al. 2014). Specifically, UV-irradiated TiO_2 produces H_2O_2 in aqueous solutions (Pappas & Fischer 1975; Konaka et al. 1999). When exposed to UV-radiation, TiO_2 photochemically generates e^-, which contributes to the reduction of O_2 into H_2O_2, as seen below, in Eq. 1 (Burek et al. 2019):

$$O_2 \xrightarrow{+e^-} \cdot O_2^- \xrightarrow{+H^+} \cdot HO_2 \xrightarrow{+e^-} \cdot HO_2^- \xrightarrow{+H^+} H_2O_2 \quad (1)$$

Subsequently, H_2O_2 can either be re-oxidized to O_2 or be further reduced to water (Burek et al. 2019).

These adverse effects have led lawmakers throughout the world to take different regulatory actions (Amenta et al. 2015; Gupta & Xie 2018). The World Health Organization has classified the carcinogenicity of TiO_2 into group 2B, deeming it "possibly carcinogenic to humans" (World Health Organization 2019). Furthermore, the European Chemicals Agency is seriously considering classifying TiO_2 as a class 1B carcinogen, deeming it "presumed to have carcinogenic potential for humans" (ANSES 2016; European Chemicals Agency 2017). The US Food and Drug Administration mandates that TiO_2 makes 1.0% or less of food by weight (U.S. Food and Drug Administration 2019) while the US National Institute for Occupational Safety and Health has recommended that TiO_2 be classified as a potential occupational carcinogen and that exposure be limited to 0.2 mg m^{-3} (National Institute for Occupational Safety and Health 2011).

Moreover, photocatalysis of TiO_2 may be influenced by common, nearly ubiquitous environmental oxyanions in soil porewaters, including nitrate and phosphate). While the TiO_2 photocatalytic reactions have been studied extensively in basic research, how environmentally relevant conditions (e.g. ligand interaction) affect its photoreactivity is not well understood. Researchers previously reported that at pH 7.9, large concentrations (5–25 mmol L^{-1}) of a common ligand, phosphate (P), decreased hydroxyl radical (·OH) generation by TiO_2 in freshwaters while nitrate decreased·OH generation to a lesser extent (Budarz et al. 2017). Others have concluded that P adsorption promoted the photocatalytic degradation of organic compounds bound weakly to TiO_2 while also inhibiting degradation of strongly sorbed organic compounds (Zhao et al. 2008). Phosphorus adsorption accelerated organic contaminant degradation at pH 6.2 in another study (Long et al. 2017). Furthermore, the presence of large concentrations of P (≥200 mM) under above neutral pH conditions boosted H_2O_2 production by TiO_2 (Xiong et al. 2018; Burek et al. 2019).

The purpose of the present study was to investigate the effect of common ligands (e.g. nitrate and phosphate) on the generation of H_2O_2 by UV-irradiated TiO_2. The results should have implications for better assessing the toxicity of TiO_2 in the aquatic and terrestrial environment. The consideration of lower, environmentally relevant nitrate and phosphate concentrations (i.e. 50 μM, 100 μM, 250 μM) and various pH conditions (4.00 ± 0.02 and 8.00 ± 0.02) differentiate the present study from previous ones. The hypothesis was that specific adsorption of P will suppress H_2O_2 production by UV-irradiated TiO_2 while the non-specific adsorption of nitrate will not interfere with the photoreactivity of TiO_2.

MATERIALS AND METHODS

Materials

All reagents were American Chemical Society (ACS) grade and all solutions were prepared using ultrapure water.

Nanopowder TiO_2 (Nanostructured and Amorphous Materials, Inc., Katy, Texas, USA) and anatase 99+% with a Brunauer, Emmett, and Teller (BET) surface area of 60 m^2 g^{-1} (Nanostructured & Amorphous Materials, Inc., Texas, USA) were used in this study. Powder X-ray diffraction (XRD) was performed on TiO_2 using a Siemens-Bruker D5000 XRD System (Bruker Corporation, Billerica, Massachusetts, USA). The voltage was adjusted to 40.0 kV and the current to 30.0 mA. The XRD angle ranged from 10 to 90°2θ, in accordance with previous studies (Sakthivel et al. 2003; Djerad et al. 2004; Anandan et al. 2008; Kathiravan & Renganathan 2009; Ravichandran et al. 2010). Furthermore, the scan speed was set at 1.2°2θ min^{-1} (Djerad et al. 2004; Ravichandran et al. 2010). The 2θ position and intensity ratio of each peak on the collected spectra were compared to an anatase TiO_2 reference pattern from the International Center for Diffraction Data (ICDD 1971).

Scanning electron microscopy (SEM) analysis was conducted on TiO_2, using a Hitachi S-4700 High Resolution SEM. Because of its low conductivity, the sample was coated with gold-palladium (Au-Pd) before analysis. The conditions of the analysis included an accelerating voltage of 15.0 kV, an emission current of 10 μA, and magnification of 90,032. After the image was captured, the diameters of ~20 individual TiO_2 particles were measured and averaged.

The zeta potential and particle size of the TiO_2 was determined using a Malvern Zetasizer (Malvern Instruments, Malvern, Worcestershire, UK), using laser Doppler velocimetry and dynamic light scattering (DLS) techniques, respectively. TiO_2 samples were prepared with suspension densities of 0.1 g L^{-1} and background solution of 0.001 M NaCl and in the presence or absence of 10 μM or 25 μM NO_3^- or P, using sodium nitrate ($NaNO_3$) and sodium phosphate (Na_2HPO_4), respectively. The samples were shaken on an end-over shaker at 50 rpm for 48 h and adjusted to various

https://doi.org/10.1007/s42860-019-00039-8 Published online by Cambridge University Press

pH conditions, using 0.01 M HCl and NaOH. The refractive index of 2.488 was used (Zhang et al. 2011). Prior to the measurements, the zetasizer was calibrated with a polystyrene latex standard.

Methods

Adsorption of Phosphate and Nitrate by TiO_2 TiO_2 suspensions (suspension density: 1 g L^{-1}) were prepared in 0.001 M NaCl (Fisher Scientific International, Inc., Fair Lawn, New Jersey, USA) and immediately sonicated for 30 s. The suspensions were kept in the dark at ambient temperature on a stir plate at 300 rpm for 24 h. The pH values of the solutions were adjusted to 4.00 ± 0.02 or 8.00 ± 0.02, using 0.01 M HCl (Fisher Scientific International, Inc., Fair Lawn, New Jersey, USA) and NaOH (Fisher Scientific International, Inc., Fair Lawn, New Jersey, USA). After the pH had stabilized, Na_2HPO_4 (Fisher Scientific International, Inc., Fair Lawn, New Jersey, USA) also prepared in 0.001 M NaCl and adjusted to pH 4.00 ± 0.02 or 8.00 ± 0.02, was added to the treatment solutions to bring the final P concentrations of the eight samples to 0, 25, 50, 75, 100, 150, 200, and 250 μM, respectively. The solutions were mixed on a reciprocal shaker at 80 rpm, and aliquots of 10 mL were removed at 48 h and passed through a 0.2 μm polyvinylidene fluoride (PVDF) syringe filter. Preliminary centrifugation experiments of filtrate showed that quantifiable nanoparticles did not pass through the filter. Solution P concentrations were measured colorimetrically using the molybdenum blue method (Murphy & Riley 1962). The same procedure was carried out to determine nitrate adsorption, except $NaNO_3$ (Fisher Scientific International, Inc., Fair Lawn, New Jersey, USA) was added to bring the concentration of the samples to 0, 50, 100, 150, 200, and 250 μM, respectively. Nitrate concentrations were determined using UV spectrometry at 220 nm (Patey et al. 2008).

UV-irradiation of TiO_2 and H_2O_2 Determination TiO_2 solutions (suspension density: 1 g L^{-1}) were prepared in 0.001 M NaCl and 10% 2-propanol (VWR, Radnor, Pennsylvania, USA) and adjusted to pH 4.00 ± 0.02 or 8.00 ± 0.02, as described above. The addition of 2-propanol optimized the analytical determination of H_2O_2 by providing additional e^- for the reduction of O_2 to H_2O_2 and suppressing H_2O_2 degradation (Burek et al. 2019). The reaction vessels, 250-mL beakers wrapped in aluminum foil, were filled with 100 mL of TiO_2 solution and placed on a magnetic stir plate set to 350 rpm. A 60 W UV-A light bulb (Feit Electric Company, Pico Rivera, California, USA) (λ: 320–400 nm) was positioned 5.5 cm above the solution surface, which had an area of 36.32 cm^2. Aliquots of 3 mL were removed from the samples at 0, 1, 5, 10, 15, 20, 30, 40, 60, 80, and 100 min and filtered through the 0.2 μm PVDF syringes. Immediately following filtration, the process of H_2O_2 determination was carried out on the aliquots, as described below.

Hydrogen peroxide was determined fluorometrically using homovanillic acid (HVA) (Acros Organics, New Jersey, USA) as a substrate (Guilbault et al. 1967, 1968; Staniek & Nohl 1999; Khosravi et al. 2013; Paital 2014). Solutions, prepared in ultrapure water, included 0.025 M tris hydroxymethyl aminomethane (tris) buffer (Macron Fine Chemicals, Center Valley, Pennsylvania, USA) , adjusted to pH 7.5; 10 U (Universal Enzyme unit in μmol/min is defined as the amount of the enzyme that catalyzes the conversion of 1 μM of substrate per min under the specified conditions) horseradish peroxidase (HRP) (Alfa Aesar, Ward Hill, Massachusetts, USA), and 125 μM HVA. To determine H_2O_2, solutions were combined in dark 15-mL vessels in the following order: 6.6. mL tris buffer, 0.9 mL HRP, 0.6 mL HVA, and 0.9 mL irradiation aliquot (Khosravi et al. 2013). Solutions were gently shaken and left to incubate for 2 h (Paital 2014). Then, each sample was transferred to a quartz fluorescence cuvette. The sample was illuminated with an excitation wavelength of 315 nm (Ci & Wang 1991; Paital 2014). Fluorescence emissions at 425 nm were measured using an Ocean Optics UV-Vis spectrophotometer (Ocean Optics, Inc., Largo, Florida, USA).

Prior to measuring the H_2O_2 concentration of irradiated samples, H_2O_2 polynomial standard curves were prepared, using 0–15 μM H_2O_2 standards. All H_2O_2 standards were made in 0.001 M NaCl and 10% 2-propanpol. The effect of background oxyanions on H_2O_2 measurements was tested by making additional standard curves using 50, 100, and 250 μM Na_2HPO_4 and 50, 100, and 250 μM $NaNO_3$ background solutions.

Kinetic and Statistical Analyses To analyze the rate of H_2O_2 production under the different pH and oxyanion conditions, time vs H_2O_2 data for each treatment were substituted into the logarithmic regression curve (i.e. $y = a \cdot \ln(x) + b$) and the statistical fitting parameters were determined.. At a given time x, H_2O_2 increased at a rate of $a{\cdot}x^{-1}$ μM min^{-1}. Coefficients of determination (R^2 values) were calculated for each regression curve. The H_2O_2 data were analyzed using two sample t-tests to determine if the population means of H_2O_2 varied significantly at 100 min based on treatment effect (i.e. the presence or absence of nitrate or phosphate).

RESULTS

TiO_2 Characterization

Various analyses were utilized to characterize TiO_2. The particle size of TiO_2 (0.1 g L^{-1}) in 0.001 M NaCl, measured by DLS, was 1040.67 ± 107.30 nm at pH 4.00 ± 0.05 and 808.57 ± 76.15 nm at pH 8.00 ± 0.05 (Fig. 1a). In 10 μM P, the particle size of TiO_2 was 2071.67 ± 186.92 nm at pH 4.00 ± 0.05 and 764.73 ± 7.81 nm at pH 8.00 ± 0.05. In 25 μM P, the particle size of TiO_2 was 2141.67 ± 189.87 nm at pH 4.00 ± 0.05 and 498.00 ± 28.52 nm at pH 8.00 ± 0.05.

XRD patterns of the TiO_2 are shown in Fig. 1b. The XRD reflections (12.65, 18.47, 24.02, 26.94, 27.53, 31.34, 70.29, 35.14, 37.043, and 41.34°2θ) confirmed the presence of anatase. A SEM image of anatase TiO_2 powder revealed that the average individual particle size was 35.89 ± 4.18 nm (n = 19) (Fig. 1c).

https://doi.org/10.1007/s42860-019-00039-8 Published online by Cambridge University Press

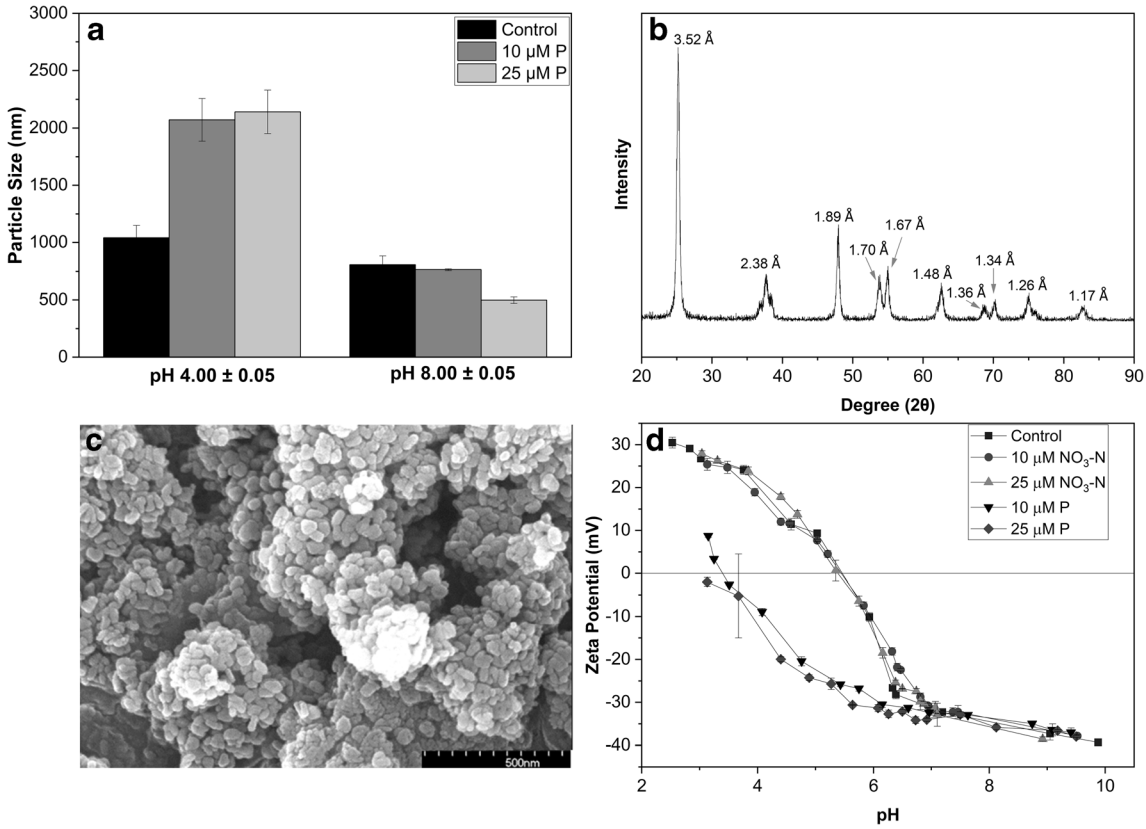

Fig. 1. Characterization of TiO_2: (**a**) particle size diameter (nm) of TiO_2 (0.1 g L^{-1}) in 0.001 M NaCl, as affected by pH and phosphate concentration; (**b**) X-ray diffraction pattern of anatase TiO_2 powder, with *d*-spacing values (Å) displayed over major peaks; (**c**) SEM image of anatase TiO_2 powder; and (**d**) zeta potential (mV) of TiO_2 (0.1 g/L) in 0.001 M NaCl in the presence and absence of phosphate and nitrate, as affected by pH (n = 3).

Zeta Potential of TiO_2 in the Presence and Absence of Oxyanions

From approximately pH 3 to 9.5, the zeta potential of TiO_2 (0.1 g L^{-1}) in 0.001 M NaCl followed very similar trends in the presence of 10 μM and 25 μM nitrate and the absence of any oxyanion ligands (Fig. 1d). For instance, the zeta potential was 11.42 ± 1.34 mV at pH 4.58 in the control, 11.67 ± 0.42 mV at pH 4.55 in 10 μM nitrate, and 13.73 ± 0.91 mV at pH 4.69 in 25 μM nitrate. The isoelectric point (IEP) occurred at around pH 5.5 in all three samples.

In the presence of 10 μM and 25 μM P, however, the zeta potential of TiO_2 deviated greatly and was much smaller compared to the other conditions from approximately pH 3 to 7. For instance, the zeta potential was –20.43 ± 1.07 mV at pH 4.76 in 10 μM P and –19.97 ± 0.58 mV at pH 4.40 in 25 μM P. In 10 μM P, the IEP of TiO_2 shifted to ~pH 3.25 while, in 25 μM P, the isoelectric point occurred at a pH lower than that of the most acidic sample. Nevertheless, at ~pH 7, the zeta potential of TiO_2 in both P concentrations became similar. At pH 9.15 ± 0.23, the zeta potential of TiO_2 in all conditions averaged –37.34 ± 0.89 mV.

Adsorption of Phosphate and Nitrate at the TiO_2–Water Interface

Adsorption of P by TiO_2 was greater at pH 4.00 ± 0.02, than at pH 8.00 ± 0.02. This was anticipated, as the positively charged TiO_2 attracts negatively charged P (Connor & McQuillan 1999). At pH 8.00 ± 0.02, the surface of TiO_2 is negatively charged, weakening this attraction. The trend line of C_{eq} vs adsorbed q for P (Fig. 2A) followed $y = 0.261 \ln(x) + 2.322$ ($R^2 = 0.9647$) at pH 4.00 ± 0.02 and $y = 0.110 \ln(x - 0.015) + 1.331$ ($R^2 = 0.9950$) at pH 8.00 ± 0.02.

Conversely, adsorption of nitrate by TiO_2 was low at pH 4.00 ± 0.02 and did not occur at pH 8.00 ± 0.02. At pH 4.00 ± 0.02, the trend line of C_{eq} vs adsorbed q for nitrate followed $y = 9.097 x^2 - 0.00601 x + 0.00165$ ($R^2 = 0.9043$) (Fig. 2b).

H_2O_2 Generation by UV-Irradiated TiO_2

UV-irradiated TiO_2 generated H_2O_2 to different degrees, depending on pH and the type and concentration of oxyanion ligand (Fig. 3; Table 1). In the control at pH 4.00 ± 0.02, H_2O_2 increased at a rate of $4.1494 x^{-1}$ μM min^{-1} and reached 18.61 μM at 100 min. The addition of P suppressed this production. At pH 4.00 ± 0.02, the rates of H_2O_2 generation were $1.76 x^{-1}$ μM min^{-1} in the presence of 50 μM P, $0.84 x^{-1}$ μM min^{-1} in the presence of 100 μM P, and $1.99 x^{-1}$ μM min^{-1} in the presence of 250 μM P. H_2O_2 reached 8.70 μM, 5.38 μM, and 9.85 μM at 100 min in 50 μM P, 100 μM P, and 250 μM P, respectively. After 100 min of irradiation, H_2O_2 was significantly ($p < 0.01$) less in the presence of P compared to its absence.

https://doi.org/10.1007/s42860-019-00039-8 Published online by Cambridge University Press

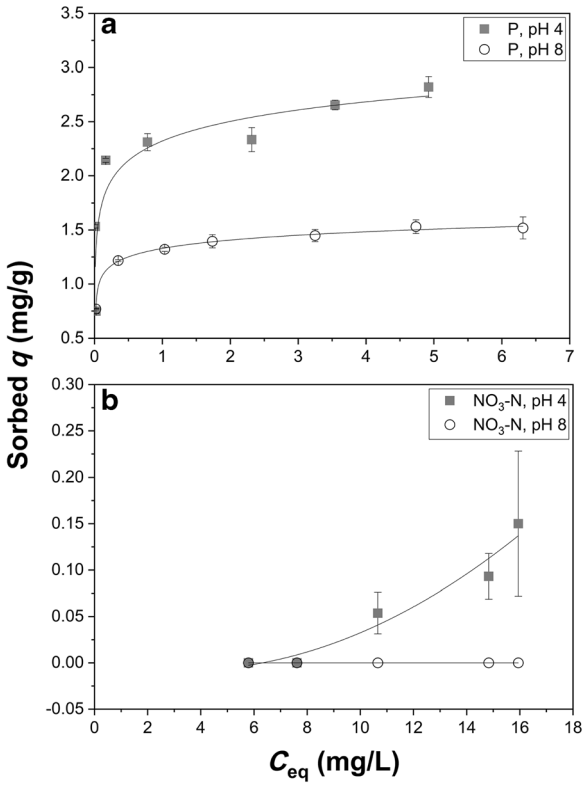

Fig. 2. Adsorption of (**a**) phosphate and (**b**) nitrate by TiO_2 (1 g L^{-1}) in 0.001 M NaCl, as affected by pH (n = 3).

Compared to P, the addition of nitrate did not cause the same inference in photocatalysis. At pH 4.00 ± 0.02, the rates of H_2O_2 generation were 4.15 x^{-1} μM min^{-1} in the presence of 50 μM nitrate, 4.19 x^{-1} μM min^{-1} in the presence of 100 μM nitrate, and 4.76 x^{-1} μM min^{-1} in the presence of 250 μM nitrate. At 100 min, H_2O_2 reached 22.98, 19.91, and 22.44 μM in 50 μM nitrate, 100 μM nitrate, and 250 μM nitrate, respectively. After 100 min of irradiation, H_2O_2 was not significantly different in the presence of nitrate compared to its absence.

At pH 8.00 ± 0.02, H_2O_2 concentration increased at markedly lower rates. In the control, H_2O_2 yield followed 0.99 x^{-1} μM min^{-1} and hit 5.79 μM at 100 min. In the presence of nitrate, H_2O_2 similarly reached 6.29, 5.58, and 5.53 μM, at 100 min in 50 μM nitrate, 100 μM nitrate, and 250 μM nitrate, respectively. The production follows the trends of 1.1430 x^{-1} μM min^{-1} in 50 μM nitrate, 1.1081 x^{-1} μM min^{-1} in 100 μM nitrate, and 0.97 x^{-1} μM min^{-1} in 250 μM nitrate. After 100 min of irradiation, H_2O_2 was not significantly different in the presence of nitrate compared to its absence.

In the presence of P at pH 8.00 ± 0.02, H_2O_2 grew at rates of 2.02 x^{-1} μM min^{-1}, 2.08 x^{-1} μM min^{-1}, and 1.51 x^{-1} μM min^{-1} and reached 10.04, 10.48, and 8.11 μM at 100 min in 50 μM P, 100 μM P, and 250 μM P, respectively. After 100 min of irradiation, H_2O_2 was significantly ($p < 0.01$) greater in the presence of P compared to its absence.

DISCUSSION

Physicochemical Properties of TiO_2

Physicochemical properties of TiO_2 were studied using XRD, SEM, and zeta potential analyses. No differences were observed when the measured XRD pattern was compared to the anatase TiO_2 reference from the ICDD database (ICDD 1971), confirming that the TiO_2 used in the present study was in fact anatase (ICDD 1971). SEM analysis revealed that the diameter of the particles of the TiO_2 powder was larger at 35.89 ± 4.18 nm (n = 19) than the size advertised by the vender (i.e. 10 nm). Furthermore, the SEM image illustrated the aggregation of the dry powder into large clusters, which is consistent with previous characterizations (French et al. 2009; Yin et al. 2012).

The zeta potential values of the control aligned with those reported previously for TiO_2 under similar conditions (Nelson et al. 2000; Dutta et al. 2004; Kataoka et al. 2004; Kim & Choi 2011; Wan et al. 2016). Below pH 5.5, TiO_2 became increasingly positively charged as the surface became more and more protonated (i.e. $TiOH_2^+$) (Kataoka et al. 2004). The reverse was true above pH 5.5, as the surface became deprotonated (i.e. TiO^-) (Kataoka et al. 2004). Moreover, in the presence of P, the zeta potential and IEP of TiO_2 shifted significantly downward due to the specific adsorption of P (Nelson et al. 2000; Wan et al. 2016).

The Effect of Nitrate on H_2O_2 Generation by UV-Irradiated TiO_2

H_2O_2 generation by UV-irradiated TiO_2 was similar between the control and nitrate treatments at both pH 4.00 ± 0.02 and 8.00 ± 0.02, while adsorption of nitrate by TiO_2 was minimal to zero. Nitrate is considered an indifferent ligand because it does not specifically interact with TiO_2 (Budarz et al. 2017). This lack of specific interaction between nitrate and TiO_2 was supported by zeta potential measurements, in which differences were not discernible between the control TiO_2 and the TiO_2 in 10 and 25 μM nitrate from pH 3 to 9.5. Consequently, the presence of nitrate did not effectively hinder or interfere with the ability of TiO_2 to produce H_2O_2 photochemically.

The Effect of Phosphate on H_2O_2 Generation by UV-Irradiated TiO_2

Phosphate strongly adsorbs to TiO_2, including the anatase form used in the present study, through inner-sphere monodentate and bidentate complexes (Hadjiivanov et al. 1989; Connor & McQuillan 1999; Zhao et al. 2008; Alshameri et al. 2014). Past infrared spectroscopic studies revealed that multinuclear complexation of P at the TiO_2 surfaces dominates (Connor & McQuillan 1999; Gong 2001; Ronson & McQuillan 2002).

Throughout the irradiation, adsorption of P by TiO_2 remained relatively constant under both acidic and alkaline conditions. Within the eleven aliquots taken from 0 to 100 min, aqueous P averaged 0.54 ± 0.46 μM at pH 4 in the 50 μM treatment, 22.23 ± 0.91 μM at pH 4 in the 100 μM treatment, 217.63 ± 2.15 μM at pH 4 in the 250 μM treatment, 23.74 ±

https://doi.org/10.1007/s42860-019-00039-8 Published online by Cambridge University Press

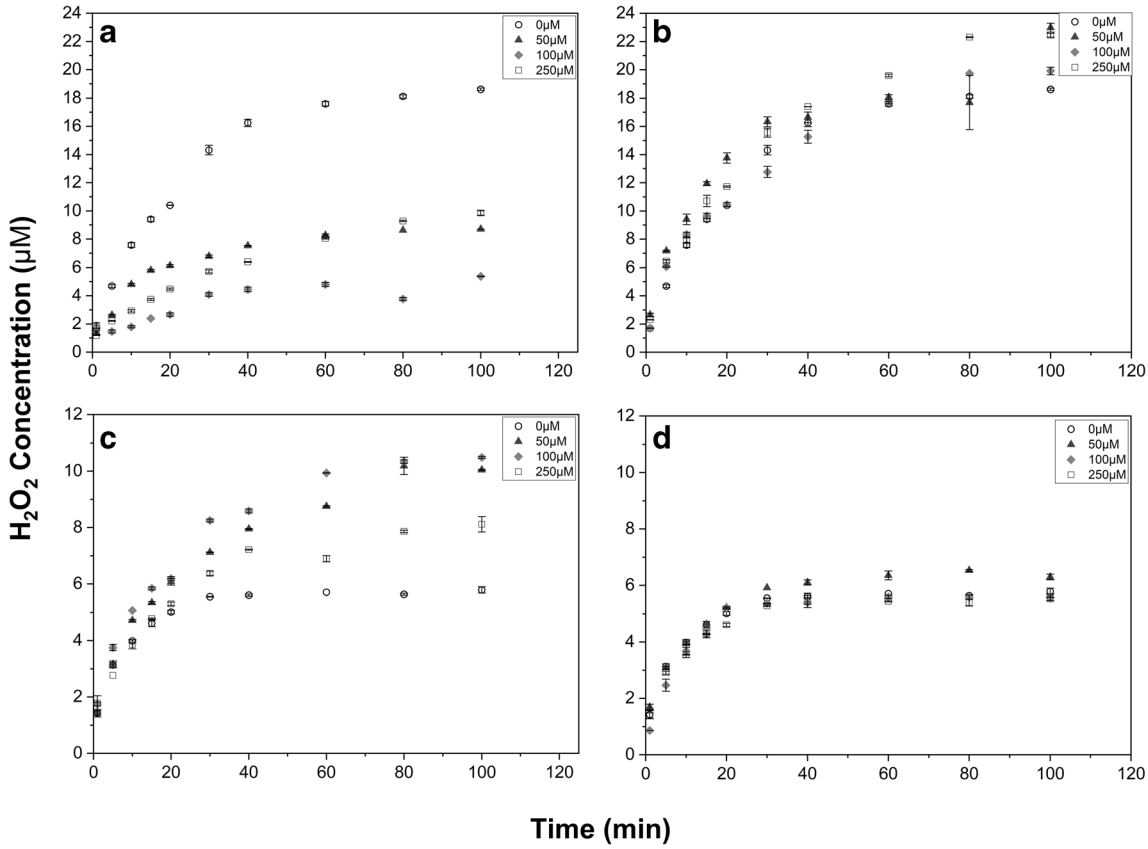

Fig. 3. H_2O_2 generation by UV-irradiated nano TiO_2 over the course of 100 min, as affected by various concentrations of (**a**) phosphate at pH 4, (**b**) nitrate at pH 4, (**c**) phosphate at pH 8, and (**d**) nitrate at pH 8 (n = 2)

1.97 μM at pH 8 in the 50 μM treatment, 70.52 ± 0.73 μM at pH 8 in the 100 μM treatment, and 224.13 ± 5.03 μM at pH 8 in the 250 μM treatment. Across the treatments, aqueous P varied, on average, 1.88 μM P during the 100 min irradiations.

The effects of P adsorption by TiO_2 photoreactivity were more complex than nitrate and varied with pH. On one hand, much adsorption of P by TiO_2 at pH 4.00 ± 0.02 corresponded to suppressed H_2O_2 generation. After 100 min of UV-irradiation, H_2O_2 was more than three times less in the presence of 100 μM P than in the absence of P. On the other hand, comparatively less adsorption of P by TiO_2 at pH 8.00 ± 0.02 corresponded to enhanced H_2O_2 production. After 100 min of UV-irradiation, H_2O_2 was nearly two times greater in the presence of 100 μM P than in the absence of P. These results can be explained by the contrasting behavior of suspended TiO_2 and H_2O_2 degradation under the different pH conditions.

Adsorbed P caused a shift in the behavior of suspended TiO_2. At pH 4.00 ± 0.05, the particle size of TiO_2 was approximately two times larger in the presence of 10 μM and 25 μM P than in the control. This is consistent with past research, which demonstrated that the adsorption of P (>50 μM) by TiO_2 led to its aggregation at pH ~3, which is lower than the IEP of the pure solid, 6.3 (Wan et al. 2016). Conversely, at pH 8.00 ± 0.05, the particle size of TiO_2 in the presence of 10 μM and 25 μM P was smaller than in the control. Past researchers have similarly observed that the adsorption of P (>50 μM) by TiO_2 under neutral to alkaline conditions (i.e. pH 7.0 and 7.9) facilitates the dispersion (Wan et al. 2016; Budarz et al. 2017).

In the present work, specific adsorption of P at pH 4.00 ± 0.02 caused the TiO_2 to aggregate and, thus, reduced its ability to generate H_2O_2 photochemically under all three concentrations (Connor & McQuillan 1999; Fujishima et al. 2008; Budarz et al. 2017). Inner-core particles within TiO_2 aggregates will not be as accessible as outer-core particles. The degree to which H_2O_2 production was suppressed correlated positively with the magnitude of P adsorption (100 μM > 50 μM > 250 μM) during irradiation. Previous studies confirmed that the aggregation of nano-TiO_2 reduces its photoreactivity, due to the reduction of reactive surface area and photon penetration (Maira et al. 2000; Hotze et al. 2010; Jassby et al. 2012). Thus, the presence of P reduced the production of H_2O_2 by UV-irradiated TiO_2 at pH 4.00 ± 0.02.

Conversely, at pH 8.00 ± 0.02, greater H_2O_2 was produced in the presence of P than in its absence. Interestingly, the extent to which H_2O_2 production was enhanced correlated with the degree of P adsorption (50 μM ~ 100 μM > 250 μM) during irradiation. The degradation of H_2O_2 at pH 8.00 ± 0.02 was approximately three times greater than at pH 4.00 ± 0.02 (Burek et al. 2019). However, under alkaline conditions, the adsorption of P by TiO_2 suppressed the adsorption of H_2O_2

https://doi.org/10.1007/s42860-019-00039-8 Published online by Cambridge University Press

Table 1. H_2O_2 generation rates, where x = time, in min, by UV-irradiated nano TiO_2, as affected by pH and oxyanion type and concentration. Solutions were prepared in 0.001 M NaCl and 10% 2-propanol, in addition to the oxyanion solutions below, and then adjusted to the specified pH

Solution pH	Solution background	H_2O_2 generation rate (μM min^{-1})	H_2O_2 (μM) vs time (min) trendline	R^2
4.00 ± 0.02	Control Phosphate	4.1494 x^{-1}	y = 4.1494ln(x) – 0.4968	0.9465
	50 μM	1.7566 x^{-1}	y = 1.7566ln(*x*) + 0.8316	0.972
	100 μM	0.8354 x^{-1}	y = 0.8354ln(x) + 0.7789	0.7048
	250 μM	1.9921 x^{-1}	y = 1.9921ln(x) – 0.5531	0.8774
	Nitrate			
	50 μM	4.1524 x^{-1}	y = 4.1524ln(x) + 1.2932	0.9515
	100 μM	4.1865 x^{-1}	y = 4.1865ln(x) – 0.3143	0.9508
	250 μM	4.7617 x^{-1}	y = 4.7617ln(x) – 0.5476	0.9369
8.00 ± 0.02	Control Phosphate	0.9883 x^{-1}	y = 0.9883ln(x) + 1.7009	0.9478
	50 μM	2.0150 x^{-1}	y = 2.0150ln(x) + 0.4758	0.9624
	100 μM	2.0753 x^{-1}	y = 2.0753ln(x) + 0.8366	0.961
	250 μM	1.5056 x^{-1}	y = 1.5056ln(x) + 1.0102	0.9481
	Nitrate			
	50 μM	1.1430 x^{-1}	y = 1.1430ln(x) + 1.5924	0.9598
	100 μM	1.1081 x^{-1}	y = 1.1081ln(x) + 1.0997	0.9274
	250 μM	0.9655 x^{-1}	y = 0.9655ln(x) + 1.5151	0.9489

onto TiO_2 and, thus, hindered its photocatalytic degradation, enabling greater aqueous H_2O_2 accumulation in the presence of P than in its absence. This phenomenon has been documented by several researchers (Moon et al. 2014; Xiong et al. 2018). Moreover, the dispersion of TiO_2 caused by P adsorption under alkaline conditions optimized its photoreactivity. Consequently, the presence of P increased aqueous H_2O_2 at pH 8.00 ± 0.02.

Environmental Implications and Uncertainties

The presence of ≥50 μM P at pH 4.00 ± 0.02 facilitated the aggregation of TiO_2, reducing its photoreactivity and ability to produce H_2O_2. Because P is nearly ubiquitous within porewaters and surface waters throughout the world, TiO_2 toxicity in terrestrial environments, under acidic conditions, may be of less concern than originally thought. However, water-soluble P varies widely from <1 to 1000 μM (Fried & Broeshart 1967; Sharpley & Smith 1989), so the extent of this suppression by P in soil environments likely varies widely. At the same time, P enhanced H_2O_2 generation at pH 8.00 ± 0.02 because P adsorption reduced the degradation of H_2O_2.

Additionally, dissolved nitrate was up to 10^3 times more prevalent in soil pore waters than P (Fried & Broeshart 1967) and did not effectively suppress or increase H_2O_2 production. Lastly, the effects of other compounds (e.g. other anions, organic compounds, colloids) commonly found in the soil matrix and their complex interactions on the photochemistry of TiO_2 are not yet understood and should be evaluated further. Thus, many uncertainties remain regarding the extent of ROS generation by TiO_2 in terrestrial and aquatic environments.

CONCLUSIONS

The ability of nano-TiO_2 to generate reactive oxygen species under UV light exposure raises concerns about its potentially adverse effects in soil, where agricultural applications and the disposal of consumer products have enabled its accumulation. In the present study, the production of H_2O_2 by UV-irradiated TiO_2 was monitored in the presence and absence of common environmental oxyanion ligands (i.e. nitrate and P) of different concentrations under acidic and alkaline conditions. At pH 4.00 ± 0.02, aggregation, caused by the specific adsorption of P onto TiO_2, suppressed the generation of H_2O_2. Conversely, adsorption of P at pH 8.00 ± 0.02 reduced H_2O_2 degradation, enabling higher H_2O_2 accumulation in solution. Nitrate, which does not specifically interact with TiO_2, did not affect the photoreactivity of TiO_2 at pH 4.00 ± 0.02 or 8.00 ± 0.02. The present work provided evidence that P positively or negatively influences TiO_2 photoreactivity at concentrations that are environmentally relevant in soil porewaters, depending on pH, while these same small concentrations of nitrate do not influence the photoreactivity of TiO_2.

ACKNOWLEDGEMENTS

The authors gratefully acknowledge the United States Department of Agriculture (Hatch #1002831-ILLU-875-939) for supporting this project financially.

Compliance with Ethical Standards

Conflict of Interest

The authors declare that we have no conflict of interest.

https://doi.org/10.1007/s42860-019-00039-8 Published online by Cambridge University Press

REFERENCES

Alshameri, A., Yan, C., & Lei, X. (2014). Enhancement of phosphate removal from water by TiO_2/Yemeni natural zeolite: Preparation, characterization and thermodynamic. *Microporous and Mesoporous Materials, 196*, 145–157.

Amenta, V., Aschberger, K., Arena, M., Bouwmeester, H., Botelho Moniz, F., Brandhoff, P., Gottardo, S., Marvin, H. J. P., Mech, A., Quiros Pesudo, L., Rauscher, H., Schoonjans, R., Vettori, M. V., Weigel, S., & Peters, R. J. (2015). Regulatory aspects of nanotechnology in the agri/feed/food sector in EU and non-EU countries. *Regulatory Toxicology and Pharmacology, 73*, 463–476.

Anandan, S., Sathish Kumar, P., Pugazhenthiran, N., Madhavan, J., & Maruthamuthu, P. (2008). Effect of loaded silver nanoparticles on TiO_2 for photocatalytic degradation of Acid Red 88. *Solar Energy Materials and Solar Cells, 92*, 929–937.

ANSES (2016). *Proposal for Harmonised Classification and Labelling Substance Name: Titanium dioxide* (pp. 1–159). France: Maisons-Alfort pp.

Bernhardt, E. S., Colman, B. P., Hochella, M. F., Cardinale, B. J., Nisbet, R. M., Richardson, C. J., & Yin, L. (2010). An ecological perspective on nanomaterial impacts in the environment. *Journal of Environmental Quality, 39*, 1954–1965.

Budarz, J. F., Turolla, A., Piasecki, A. F., Bottero, J. Y., Antonelli, M., & Wiesner, M. R. (2017). Influence of Aqueous Inorganic Anions on the Reactivity of Nanoparticles in TiO_2 Photocatalysis. *Langmuir, 33*, 2770–2779.

Burek, B. O., Bahnemann, D. W., & Bloh, J. Z. (2019). Modeling and optimization of the photocatalytic reduction of molecular oxygen to hydrogen peroxide over titanium dioxide. *ACS Catalysis, 9*, 25–37.

Ci, Y. X., & Wang, F. (1991). Catalytic effects of peroxidase-like metalloporphyrins on the fluorescence reaction of homovanillic acid with hydrogen peroxide. *Fresenius' Journal of Analytical Chemistry, 339*, 46–49.

Connor, P. A., & McQuillan, A. J. (1999). Phosphate adsorption onto TiO_2 from aqueous solutions: an in situ internal reflection infrared spectroscopic study. *Langmuir, 15*, 2916–2921.

Djerad, S., Tifouti, L., Crocoll, M., & Weisweiler, W. (2004). Effect of vanadia and tungsten loadings on the physical and chemical characteristics of V_2O_5-WO_3/TiO_2 catalysts. *Journal of Molecular Catalysis A: Chemical, 208*, 257–265.

Drobne, D., Jemec, A., & Pipan Tkalec, Ž. (2009). In vivo screening to determine hazards of nanoparticles: Nanosized TiO_2. *Environmental Pollution, 157*, 1157–1164.

Dutta, P. K., Ray, A. K., Sharma, V. K., & Millero, F. J. (2004). Adsorption of arsenate and arsenite on titanium dioxide suspensions. *Journal of Colloid and Interface Science, 278*, 270–275.

European Chemicals Agency (2017) *Titanium dioxide proposed to be classified as suspected of causing cancer when inhaled*. Helsinki, Finland. https://echa.europa.eu/-/titanium-dioxide-proposed-to-be-classified-as-suspected-of-causing-cancer-when-inhaled.

French, R. A., Jacobson, A. R., Kim, B., Isley, S. L., Penn, L., & Baveye, P. C. (2009). Influence of ionic strength, pH, and cation valence on aggregation kinetics of titanium dioxide nanoparticles. *Environmental Science and Technology, 43*, 1354–1359.

Fried, M., & Broeshart, H. (1967) *The Soil-Plant System*. Acadamic Press, New York, NY.

Fu, P. P., Xia, Q., Hwang, H. M., Ray, P. C., & Yu, H. (2014). Mechanisms of nanotoxicity: Generation of reactive oxygen species. *Journal of Food and Drug Analysis, 22*, 64–75.

Fujishima, A., Zhang, X., & Tryk, D. A. (2008). TiO_2 photocatalysis and related surface phenomena. *Surface Science Reports, 63*, 515–582.

Gardea-Torresdey, J. L., Rico, C. M., & White, J. C. (2014). Trophic transfer, transformation, and impact of engineered nanomaterials in terrestrial environments. *Environmental Science and Technology, 48*, 2526–2540.

Ghosh, M., Bandyopadhyay, M., & Mukherjee, A. (2010). Genotoxicity of titanium dioxide (TiO_2) nanoparticles at two trophic levels: Plant and human lymphocytes. *Chemosphere, 81,* 1253–1262.

Gondikas, A. P., Von Der Kammer, F., Reed, R. B., Wagner, S., Ranville, J. F., & Hofmann, T. (2014). Release of TiO_2 nanoparticles from sunscreens into surface waters: A one-year survey at the old Danube recreational lake. *Environmental Science and Technology, 48*, 5415–5422.

Gong, W. (2001). A real time in situ ATR-FTIR spectroscopic study of linear phosphate adsorption on titania surfaces. *International Journal of Mineral Processing, 63*, 147–165.

Gottschalk, F., Sonderer, T., Scholz, R. W., & Nowack, B. (2009). Modeled Environmental Concentrations of Engineered Nanomaterials (TiO_2, ZnO, Ag, CNT, Fullerenes) for Different Regions. *Environmental Science and Technology, 43*, 9216–9222.

Guilbault, G. G., Kramer, D. N., & Hackley, E. (1967). A New Substrate for Fluorometric Determination of Oxidative Enzymes. *Analytical Chemistry, 39*, 271.

Guilbault, G. G., Brignac, P., & Zimmer, M. (1968). Homovanillic Acid as a Fluorometric Substrate for Oxidative Enzymes. Analytical Applications of the Peroxidase, Glucose Oxidase, and Xanthine Oxidase Systems. *Analytical Chemistry, 40*, 190–196.

Gupta, R., & Xie, H. (2018). Nanoparticles in Daily Life: Applications, Toxicity and Regulations. *Journal of Environmental Pathology, Toxicology and Oncology, 37*, 209–230.

Hadjiivanov, K. I., Klissurski, D. G., & Davydov, A. A. (1989). Study of phosphate-modified TiO_2 (anatase). *Journal of Catalysis, 116*, 498–505.

Hotze, E. M., Phenrat, T., & Lowry, G. V. (2010). Nanoparticle aggregation: challenges to understanding transport and reactivity in the environment. *Journal of Environmental Quality, 39*, 1909–1924.

Hu, C. W., Li, M., Cui, Y. B., Li, D. S., Chen, J., & Yang, L. Y. (2010). Toxicological effects of TiO_2 and ZnO nanoparticles in soil on earthworm Eisenia fetida. *Soil Biology and Biochemistry, 42*, 586–591.

ICDD (1971) *Anatase Titanium Oxide*. Newtown Square, PA. PDF #00-021-1272.

Jassby, D., Farner Budarz, J., & Wiesner, M. (2012). Impact of aggregate size and structure on the photocatalytic properties of TiO_2 and ZnO nanoparticles. *Environmental Science and Technology, 46*, 6934–6941.

Kataoka, S., Gurau, M. C., Albertorio, F., Holden, M. A., Lim, S. M., Yang, R. D., & Cremer, P. S. (2004). Investigation of water structure at the TiO_2/aqueous interface. *Langmuir, 20*, 1662–1666.

Kathiravan, A., & Renganathan, R. (2009). Effect of anchoring group on the photosensitization of colloidal TiO_2 nanoparticles with porphyrins. *Journal of Colloid and Interface Science, 331*, 401–407

Kavan, L., Stoto, T., Grätzel, M., Fitzmaurice, D., & Shklover, V. (1993). Quantum size effects in nanocrystalline semiconducting TiO_2 layers prepared by anodic oxidative hydrolysis of TiCl3. *Journal of Physical Chemistry, 97*, 9493–9498.

Keller, A. A., & Lazareva, A. (2013). Predicted Releases of Engineered Nanomaterials: From Global to Regional to Local. *Environmental Science and Technology Letters, 1*, 65–70.

Khosravi, A., Vossoughi, M., Shahrokhian, S., & Alemzadeh, I. (2013). Magnetic labelled horseradish peroxidase-polymer nanoparticles: A recyclable nanobiocatalyst. *Journal of the Serbian Chemical Society, 78*, 921–931.

Kim, J., & Choi, W. (2011). TiO_2 modified with both phosphate and platinum and its photocatalytic activities. *Applied Catalysis B: Environmental, 106*, 39–45.

Konaka, R., Kasahara, E., Dunlap, W. C., Yamamoto, Y., Chien, K. C., & Inoue, M. (1999). Irradiation of titanium dioxide generates both singlet oxygen and superoxide anion. *Free Radical Biology and Medicine, 27*, 294–300.

Long, M., Brame, J., Qin, F., Bao, J., Li, Q., & Alvarez, P. J. J. (2017). Phosphate Changes Effect of Humic Acids on TiO_2 Photocatalysis: From Inhibition to Mitigation of Electron-Hole Recombination. *Environmental Science and Technology, 51*, 514–521.

https://doi.org/10.1007/s42860-019-00039-8 Published online by Cambridge University Press

Ma, H., Brennan, A., & Diamond, S. A. (2012). Photocatalytic reactive oxygen species production and phototoxicity of titanium dioxide nanoparticles are dependent on the solar ultraviolet radiation spectrum. *Environmental Toxicology and Chemistry, 31*, 2099–2107.

Maira, A. J., Yeung, K. L., Lee, C. Y., Yue, P. L., & Chan, C. K. (2000). Size effects in gas-phase photo-oxidation of trichloroethylene using nanometer-sized TiO_2 catalysts. *Journal of Catalysis, 192*, 185–196.

Manke, A., Wang, L., & Rojanasakul, Y. (2013) Mechanisms of nanoparticle-induced oxidative stress and toxicity. *BioMed Research International*, https://doi.org/10.1155/2013/942916

Moon, G. H., Kim, W., Bokare, A. D., Sung, N. E., & Choi, W. (2014). Solar production of H_2O_2 on reduced graphene oxide-TiO_2 hybrid photocatalysts consisting of earth-abundant elements only. *Energy and Environmental Science, 7*, 4023–4028.

Mueller, N. C., Som, C., & Nowack, B. (2009). Exposure modeling of engineered nanoparticles. *Nanotech Conference & Expo 2009, Vol 1, Technical Proceedings, 41*, 159–162.

Murphy, J., & Riley, J. P. (1962). A modified single solution method for the determination of phosphate in natural waters. *Analytica Chimica Acta, 27*, 31–36.

National Institute for Occupational Safety and Health (2011) *Current Intelligence Bulletin 63: Occupational Exposure to Titanium Dioxide*. https://www.cdc.gov/niosh/docs/2011-160/default.html.

Nelson, B. P., Candal, R., Corn, R. M., & Anderson, M. A. (2000). Control of surface and ζ potentials on nanoporous TiO_2 films by potential-determining and specifically adsorbed ions. *Langmuir, 16*, 6094–6101.

Paital, B. (2014) A modified fluorimetric method for determination of hydrogen peroxide using homovanillic acid oxidation principle. *BioMed Research International*, 2014. https://doi.org/10.1155/2014/342958.

Pappas, P. S., & Fischer, R. M. (1975). Photo-chemistry of pigments. studies on the mechanism of chalking. *Pigment & Resin Technology, 4*, 3–10.

Patey, M. D., Rijkenberg, M. J. A., Statham, P. J., Stinchcombe, M. C., Achterberg, E. P., & Mowlem, M. (2008). Determination of nitrate and phosphate in seawater at nanomolar concentrations. *Trends in Analytical Chemistry, 27*, 169–182.

Ravichandran, L., Selvam, K., & Swaminathan, M. (2010). Highly efficient activated carbon loaded TiO_2 for photo defluoridation of pentafluorobenzoic acid. *Journal of Molecular Catalysis A: Chemical, 317*, 89–96.

Roh, J. Y., Park, Y. K., Park, K., & Choi, J. (2010). Ecotoxicological investigation of CeO_2 and TiO_2 nanoparticles on the soil nematode Caenorhabditis elegans using gene expression, growth, fertility, and survival as endpoints. *Environmental Toxicology and Pharmacology, 29*, 167–172.

Ronson, T. K., & McQuillan, A. J. (2002). Infrared Spectroscopic Study of Calcium and Phosphate Ion Coadsorption and of Brushite Crystallization on TiO_2. *Langmuir, 18*, 5019–5022.

Sajid, M., Ilyas, M., Basheer, C., Tariq, M., Daud, M., Baig, N., & Shehzad, F. (2015). Impact of nanoparticles on human and environment: review of toxicity factors, exposures, control strategies, and future prospects. *Environmental Science and Pollution Research, 22*, 4122–4143.

Sakthivel, S., Neppolian, B., Shankar, M. V., Arabindoo, B., Palanichamy, M., & Murugesan, V. (2003). Solar photocatalytic degradation of azo dye: comparison of photocatalytic efficiency of ZnO and TiO_2. *Solar Energy Materials & Solar Cells, 77*, 65–82.

Servin, A. D., Morales, M. I., Castillo-Michel, H., Hernandez-Viezcas, J. A., Munoz, B., Zhao, L., Nunez, J. E., Peralta-Videa, J. R., & Gardea-Torresdey, J. L. (2013). Synchrotron verification of TiO_2 accumulation in cucumber fruit: A possible pathway of TiO_2 nanoparticle transfer from soil into the food chain. *Environmental Science and Technology, 47*, 11592–11598.

Sharpley, A. N., & Smith, S. J. (1989). Prediction of Bioavailable Phosphorus Loss in Agricultural Runoff. *Journal of Environment Quality, 18*, 32.

Skocaj, M., Filipic, M., Petkovic, J., & Novak, S. (2011). Titanium dioxide in our everyday life; Is it safe? *Radiology and Oncology, 45*, 227–247.

Staniek, K., & Nohl, H. (1999). H_2O_2 detection from intact mitochondria as a measure for one-electron reduction of dioxygen requires a non-invasive assay system. *Biochimica et Biophysica Acta - Bioenergetics, 1413*, 70–80.

Tan, W., Peralta-Videa, J. R., & Gardea-Torresdey, J. L. (2018). Interaction of titanium dioxide nanoparticles with soil components and plants: Current knowledge and future research needs-a critical review. *Environmental Science: Nano, 5*, 257–278.

U.S. Food and Drug Administration (2019) Food and Drugs Chapter 1. Listing of Color Additives Exempt from Certification. https://www.accessdata.fda.gov/scripts/cdrh/cfdocs/cfcfr/CFRSearch.cfm?CFRPart=73.

Valant, J., Drobne, D., Sepčić, K., Jemec, A., Kogej, K., & Kostanjšek, R. (2009). Hazardous potential of manufactured nanoparticles identified by in vivo assay. *Journal of Hazardous Materials, 171*, 160–165.

Wan, B., Yan, Y., Liu, F., Tan, W., He, J., & Feng, X. (2016). Surface speciation of myo-inositol hexakisphosphate adsorbed on TiO_2 nanoparticles and its impact on their colloidal stability in aqueous suspension: A comparative study with orthophosphate. *Science of the Total Environment, 544*, 134–142.

Wang, H., Wick, R. L., & Xing, B. (2009). Toxicity of nanoparticulate and bulk ZnO, Al_2O_3 and TiO_2 to the nematode Caenorhabditis elegans. *Environmental Pollution, 157*, 1171–1177.

Weir, A., Westerhoff, P., Fabricius, L., Hristovski, K., & Von Goetz, N. (2012). Titanium dioxide nanoparticles in food and personal care products. *Environmental Science and Technology, 46*, 2242–2250.

World Health Organization, (2019) *Agents Classified by the International Agency for Research on Cancer Monographs, Volumes 1-23*. Geneva, Switzerland.

Xiong, X., Zhang, X., Liu, S., Zhao, J., & Xu, Y. (2018). Sustained production of H_2O_2 in alkaline water solution using borate and phosphate-modified Au/TiO_2 photocatalysts. *Photochemical and Photobiological Sciences, 17*, 1018–1022.

Yang, F., Hong, F., You, W., Liu, C., Gao, F., Wu, C., & Yang, P. (2006). Influences of nano-anatase TiO_2 on the nitrogen metabolism of growing spinach. *Biological Trace Element Research, 110*, 179–190.

Yin, J.-J., Liu, J., Ehrenshaft, M., Roberts, J. E., Fu, P. P., Mason, R. P., & Zhao, B. (2012). Phototoxicity of Nano Titanium Dioxides in HaCaT Keratinocytes – Generation of Reactive Oxygen Species and Cell Damage. *Toxicology and Applied Pharmacy, 263*, 81–88.

Zhang, Q., Lima, D. Q., Lee, I., Zaera, F., Chi, M., & Yin, Y. (2011). A highly active titanium dioxide based visible-light photocatalyst with nonmetal doping and plasmonic metal decoration. *Angewandte Chemie - International Edition, 50*, 7088–7092.

Zhao, D., Chen, C., Wang, Y., Ji, H., Ma, W., Zang, L., & Zhao, J. (2008). Surface Modification of TiO_2 by Phosphate: Effect on Photocatalytic Activity and Mechanism Implication. *Journal of Physical Chemistry 112*, 5993–6001.

(Received 5 June 2019; revised 5 September 2019; accepted 14 October 2019; AE: Chun-Hui Zhou)